

# KA-BAND PROPAGATION STUDIES USING THE ACTS PROPAGATION TERMINAL AND THE CSU-CHILL MULTIPARAMETER, DOPPLER RADAR

J. Beaver\*, J. Turk† and V.N. Bringi\*

Colorado State University  
Fort Collins, Colorado

## 1 INTRODUCTION

An increase in the demand for satellite communications has led to an overcrowding of the current spectrums being used - mainly at C and Ku bands. To alleviate this overcrowding, new technology is being developed to open up the Ka-band for communications use. One of the first experimental communications satellites using this technology is NASA's Advanced Communications Technology Satellite (ACTS).

In September 1993, ACTS was deployed into a geostationary orbit near 100° W longitude. The ACTS system employs two Ka-band beacons for propagation experiments, one at 20.185 GHz and another at 27.505 GHz. Attenuation due to rain and tropospheric scintillations will adversely affect new technologies proposed for this spectrum. Therefore, before being used commercially, propagation effects at Ka-band must be studied.

Colorado State University is one of eight sites across the United States and Canada conducting propagations studies; each site is equipped with the ACTS propagation terminal (APT) [1]. With each site located in a different climatic zone, the main objective of the propagation experiment is to obtain monthly and yearly attenuation statistics. Each site also has secondary objectives that are site dependent.

At CSU, the CSU-CHILL radar facility is being used to obtain polarimetric radar data along the ACTS propagation path. During the expected two to four year period of the project, it is hoped to study several significant weather events. The S-band radar data will be used to obtain Ka-band attenuation estimates and to initialize propagation models that have been developed, to help classify propagation events measured by the APT [2].

Preliminary attenuation estimates for two attenuation events will be shown here - a bright band case that occurred on May 13, 1994 and a convective case that occurred on June 20, 1994. Section 2 will detail the computations used to obtain Ka-band attenuation estimates from S-band radar data. In Section 3, results from the two events will be shown.

## 2 COMPUTATIONS

As a preliminary step in obtaining attenuation estimates

\*Colorado State University, Dept. Of Electrical Engineering, Fort Collins, CO 80523

†Naval Research Lab, 7 Grace Hopper Ave, Monterey, CA 93943

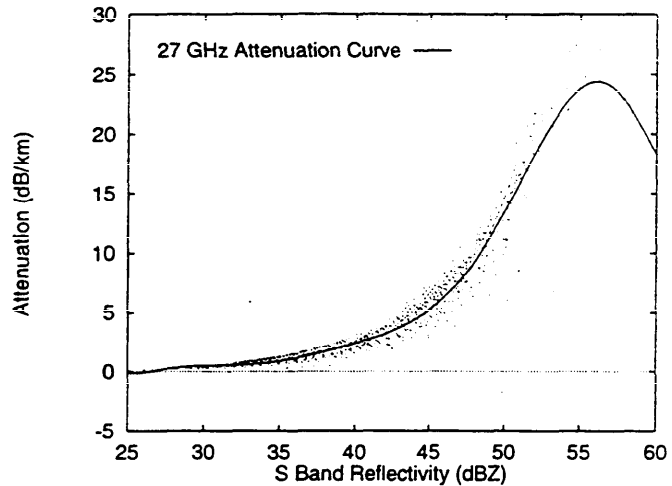


Figure 1: Attenuation for 27 GHz versus reflectivity at 3 GHz, obtained using a Mie solution for spherical particles.

for Ka-band using S-band radar data, a Mie solution for spherical water particles is used. Attenuation estimates for 20 and 27 GHz versus reflectivity at 3 GHz are obtained by varying the parameters of the gamma drop size distribution

$$N(D) = N_0 D^m e^{-\gamma D} \quad (1)$$

where

$$\gamma = \frac{3.67 + m}{D_0} \quad (2)$$

and  $N(D)$ , given in  $mm^{-1}m^{-3}$ , is the number of drops per unit volume per unit size interval,  $D$  is the equivalent drop size diameter in mm,  $N_0$  is given in  $mm^{-1}m^{-3}$ ,  $D_0$  is the median drop size in mm and  $m$  is the shape factor. Scatter plots were obtained for 20 and 27 GHz by varying the DSD parameters ( $N_0, D_0, m$ ). The attenuation curves were then computed by applying an 8<sup>th</sup> order polynomial fit to the data. The result for 27 GHz is shown in Figure 1.

Attenuation estimates at Ka-band were also obtained using specific differential phase,  $KDP$ , at S-band and are shown in Figure 2. Here a T-matrix solution was used to obtain the scattering amplitudes for oblate raindrops ranging in size from 1-8 mm. S-band  $KDP$  and specific attenuation at Ka-band were then computed from the Mueller matrix, averaged over

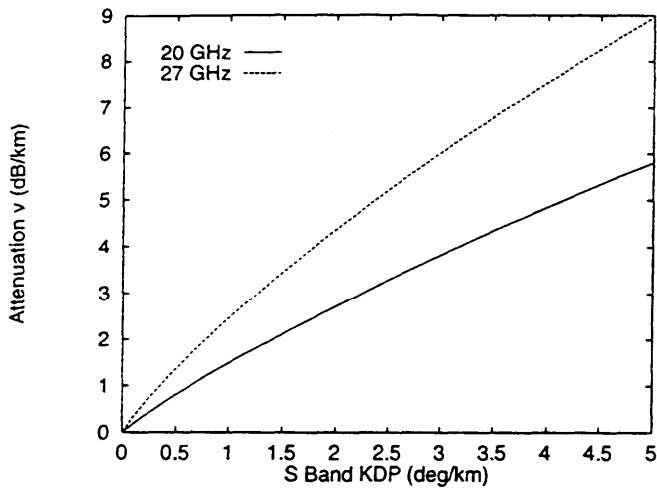


Figure 2: Attenuation for 20 and 27 GHz versus specific differential phase at 3 GHz, obtained via T-matrix and Mueller matrix solutions.

an exponential DSD ( $m = 0$ ). The attenuation curves were derived by varying the DSD parameter  $D_0$ , while  $N_0$  was fixed at  $8000 \text{ mm}^{-1} \text{ m}^{-3}$ .

### 3 RESULTS

The May 13 bright band case is examined first. Attenuation measurements taken by the CSU-APT are shown in Figure 3. A range profile of radar observables, along the propagation path, is shown in Figure 4. The horizontal reflectivity,  $Z_H$ , profile shows a well defined bright band at a height of approximately 1.93 km, with values of 40 to 45 dBZ. The increase in reflectivity is due to the aggregation of ice particles and an increase in the dielectric constant as the particles begin to melt. The differential reflectivity,  $Z_{DR}$ , profile indicates values of 0.9 to 1.2 dB in the bright band. The enhanced region of  $Z_{DR}$  can be attributed to the fact that the aggregates have reached their largest size and are becoming more oblate as they melt. The increasing dielectric constant also contributes to the increase of differential reflectivity. The cross correlation coefficient,  $\rho_{HV}$ , profile is also shown. This is at the base of the melting layer, the point just before the aggregates collapse into raindrops. Values of  $\rho_{HV}$ , in the bright band are typically .93 to .94, which indicates of a wide distribution of shapes in this region. Finally the differential phase shift upon backscatter,  $\delta$ , is shown. The presence of  $\delta$  gives an indication of large Mie particles in the melting layer. It is located between the peak values of  $Z_H$  and  $Z_{DR}$  [3].

There are three periods of time when the CSU-CHILL radar took scans along the ACTS propagation path during this event. Reflectivity, ( $Z_H$ ), measurements at 3 GHz are available at 150 m increments along the path. The corresponding 20 and 27 GHz attenuation estimates are determined from the data shown in Figure 1 and multiplied by the appropriate distance. The results using the reflectivity-attenuation curves for 20 GHz are given in Table 1, while those for 27 GHz are given in Table 2. For this particular event S-band  $KDP$  values were too small to obtain

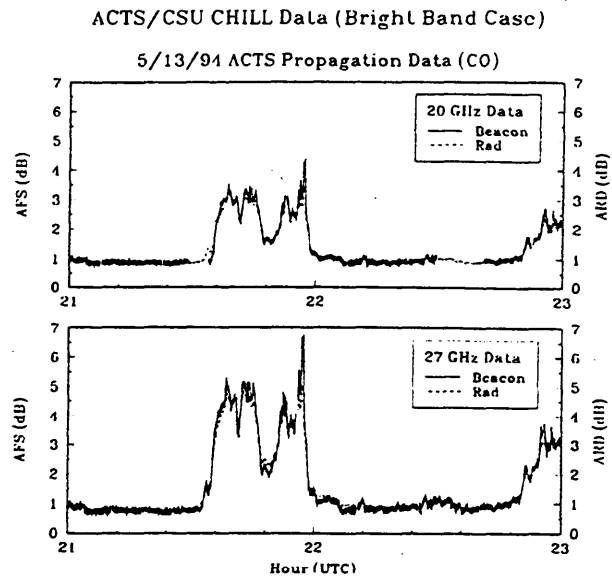


Figure 3: CSU-APT attenuation curves for May 13, 1994 bright band case.

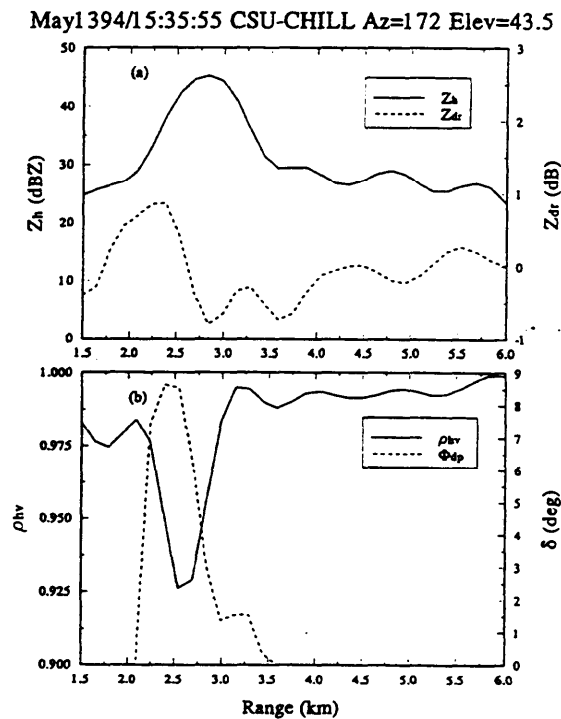


Figure 4: Range profile of  $Z_h$ ,  $Z_{DR}$ ,  $\rho_{HV}$  and  $\delta$  for the May 13, 1994 convective case.

Time (GMT)	ACTS Attn (dB)	CHILL Attn (dB)
21:35:55	2.26	2.43
21:53:00	3.06	2.01
21:55:18	2.38	2.23

Table 1: 20 GHz attenuation estimates obtained by the CSU-APT and from CSU-CHILL S-band radar data.

Time (GMT)	ACTS Attn (dB)	CHILL Attn (dB)
21:35:55	3.51	3.86
21:53:00	4.49	3.08
21:55:18	3.55	3.48

Table 2: 27 GHz attenuation comparisons obtained by the CSU-APT and from CSU-CHILL S-band radar data.

attenuation estimates.

A rain event that occurred on June 20, caused a signal loss at 27 GHz for approximately 15 minutes. The 20 GHz signal bounced in and out of lock several times, but for only very short durations. Figure 5 shows attenuation data for both the 20 and 27 GHz channels. A range profile of  $Z_h$ ,  $Z_{DR}$ ,  $\rho_{HV}$  and  $KDP$  along the propagation path is shown in Figure 6. Starting at 2 km, along the propagation path, reflectivity values are on the order of 45 dBZ. At 6.5 km  $Z_H$  reaches a maximum of 54 dBZ. Low values of  $Z_{DR}$ , combined with high reflectivity values, a dip in the cross correlation coefficient, and measurable values of specific differential phase,  $KDP$ , at 6 km indicates a region with a mixture of melting hail and raindrops along the ACTS propagation path. There were 43 radar scans taken throughout the duration of the event. Attenuation estimates from reflectivity data and  $KDP$  data are derived from these scans. The results are shown Figure 7.

As seen in Figure 7, the CSU-CHILL reflectivity derived attenuation estimates follow the attenuation measurements obtained from the APT very closely. The maximum difference is about 5 db, while for the most part the CSU-CHILL derived estimates are within 1-2 dB of those measured by the CSU-APT. The attenuation estimates derived from  $KDP$  data alone grossly underestimated the attenuation caused by this event. This may be explained by examining Figure 8, a scatter plot of the APT measured 20 GHz attenuation versus the one way differential phase measured by the CSU-CHILL radar.

One way differential phase,  $\Phi_{DP}$ , and its derivative  $KDP$  are only sensitive to the oblateness of a particle, therefore the difference seen between the maximum and minimum values of the fitted curve in Figure 8 is caused by the presence of various sizes of oblate rain drops throughout the medium. If the medium were comprised of only raindrops the y-intercept of the fitted curve would be at zero; however, if the fitted curve is extended back to  $\Phi_{DP} = 0$ , the y-intercept is at 23.97 dB. This indicates that a large amount of attenuation was due to spherical, water coated ice particles. As indicated previously, there was indeed a region of mixed phase along the propagation path, however from Figure 8 and the fact that  $KDP$  data alone grossly underestimates the attenuation is

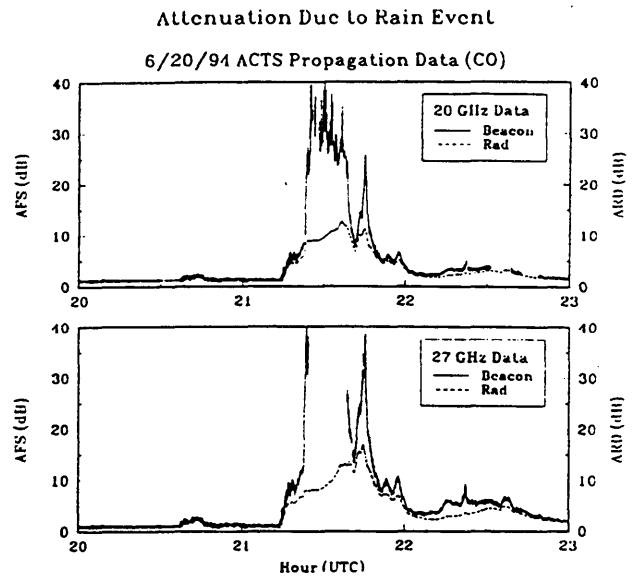


Figure 5: June 20, 1994 rain event, measured by the CSU-APT.

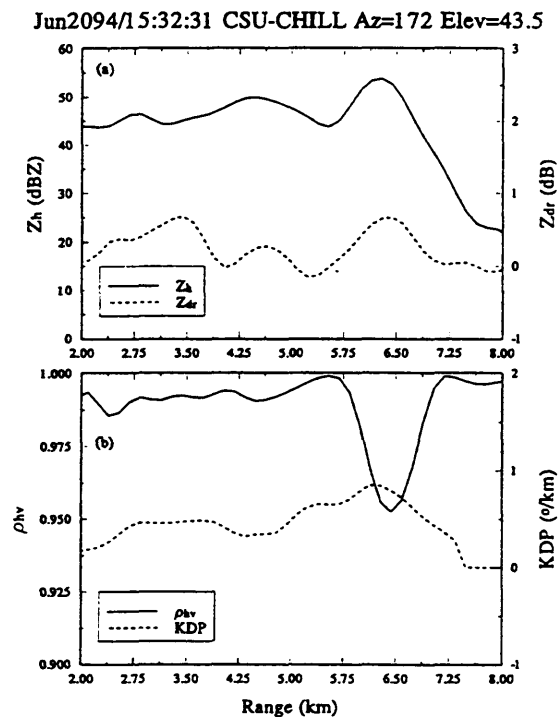


Figure 6: Range profile of  $Z_h$ ,  $Z_{DR}$ ,  $\rho_{HV}$  and  $KDP$  for the June 20, 1994 convective case.

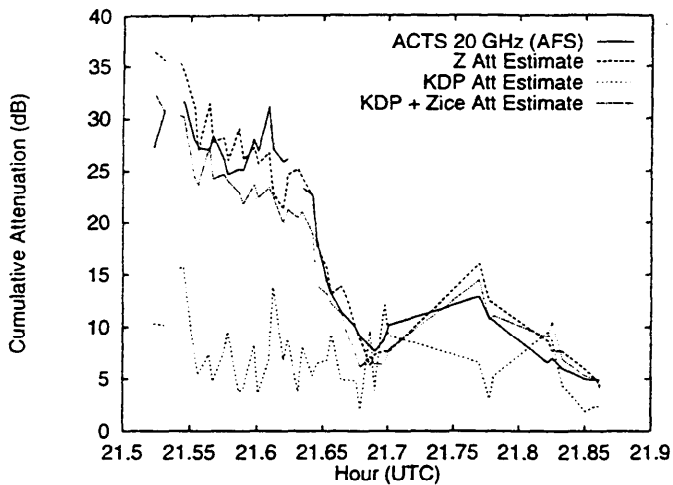


Figure 7: Comparison of measured CSU-APt attenuation and 20 GHz attenuation estimates derived from CSU-CHILL data.

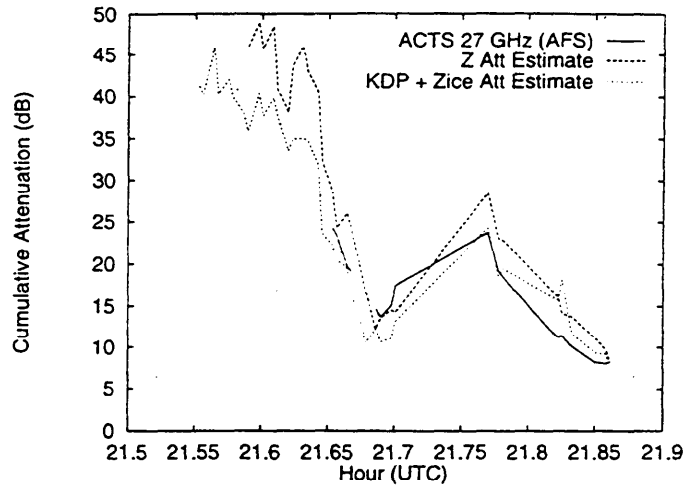


Figure 9: Comparison of measured CSU-APT attenuation and 27 GHz attenuation estimates derived from CSU-CHILL data.

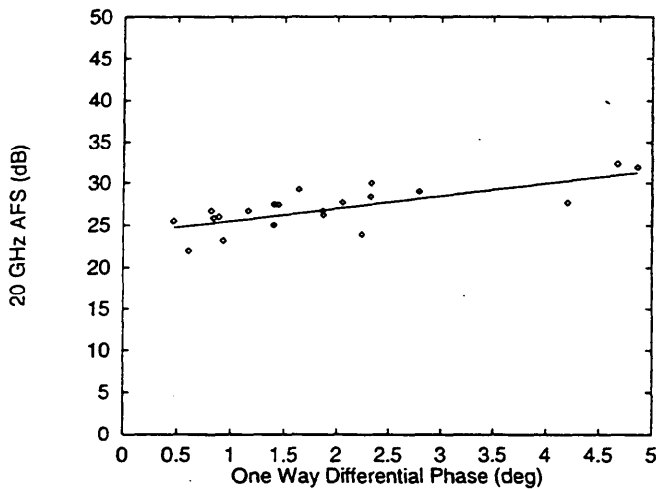


Figure 8: 20 GHz attenuation versus one way differential phase, for the June 20, 1994 convective case.

an indication that water coated ice particles could have been present throughout the propagation path during this event. Considering this to be the case, the next step is to determine the reflectivity due only to the water coated ice particles along the propagation path from the total reflectivity measured by the CSU-CHILL radar. This is done by using  $Z_{DR}$  to determine the ice fraction content in the range resolution volume at each 150 m increment along the propagation path. Once the ice fraction content is determined, the reflectivity due to the water coated ice particles is computed and used to determine the attenuation at 20 and 27 GHz due to these particles alone, while the attenuation due to the oblate raindrops is computed using  $KDP$  data.

The combined results are shown in Figure 7, while the attenuation estimates are still slightly underestimated for the most part, the CSU-CHILL derived attenuation estimates us-

ing  $KDP$  and  $Z_{ICE}$  are within 1 to 2 dB of the the attenuation values obtained by the CSU-APT. The 27 GHz results are shown in Figure 9.

While these are just preliminary results, they are very encouraging. The June 20 convective case is a good example of how the different parameters available from the CSU-CHILL radar can be used to determine the nature of precipitation particles along the propagation path. Currently, other events for which radar data is available are being analyzed, in addition to refining the methods used to obtain the attenuation estimates from S-band radar data.

## References

- [1] W. L. Stutzman, et al., "ACTS Propagation Terminal Hardware Description Report," Virginia Tech Report No. EESATCOM 93-9, June 1993.
- [2] V.N. Bringi, V. Chandrasekar and Y. Golestani, "Polarimetric Radar Measurements in Convective Storms," *Direct and Inverse Methods in Radar Polarimetry, Part 2*, 1992.
- [3] D. Zrnic, N. Balakrishnan, C. Ziegler, V.N. Bringi, K. Aydin and T. Matejka, "Polarimetric Signatures in the Stratiform Region of a Mesoscale Convective System," *Journal of Applied Meteorology*, vol. 32, April 1993.

## Acknowledgement

The authors would like to acknowledge support from NASA contract NAS3-26410. We would also like to thank Pat Kennedy, Dave Brunkow and Ken Pattison of the CSU-CHILL radar facility, for their help in collecting radar data. Finally we would like to thank David Westenhaver for his continued support in keeping the terminal operational.